ment is approximately f/2, so scattered photons whose propagation has been diverted by less than ~14° are still collected by the lens. These photons have traveled a slightly longer path through the material, and are therefore delayed somewhat.

For these samples, the product of the wave vector and the mean free path l_t is never less than ~20, so these data represent only the weak scattering regime. However, we can also fabricate strongly scattering samples, using 0.5 mm cubes of high-resistivity silicon, (n = 3.42). With these samples, it is possible to more closely approach the Ioffe-Regel criterion, $k \cdot l_t \sim 1$. These data demonstrate the possibility of using THz time-domain spectroscopy for light localization measurements.

References

1. A. Ishimaru, *Wave propagation and scattering in random media* (Academic Press, New York, 1978).
2. D.S. Wiersma, P. Bartolini, A. Lagendijk, and R. Righini, *Nature* 390, 671 (1997).
3. R. Graaff and J.J.T. Bosch, *Opt. Lett.* 25, 43 (2000).
4. R.H.J. Kop, P. de Vries, R. Sprik, and A. Lagendijk, *Phys. Rev. Lett.* 79 4369 (1997).
5. A.A. Chabanov and A.Z. Genack, *Phys. Rev. E* 56, 1338 (1997).

JMC2 **4:00 pm**

Powder Detection Using THz Imaging

Shaohong Wang,[1] Bradley Ferguson,[1,2] Carmen Mannella,[3] Derek Abbott,[2] and X.-C. Zhang,[1] [1]Department of Physics, Applied Physics and Astronomy, Rensselaer Polytechnic Institute, Troy, NY 12180, USA; [2]Department of Electrical & Electronic Engineering, Adelaide University, SA 5005, Australia; [3]Wadsworth Center, New York State Department of Health, Albany, NY 12201, Email: zhangxc@rpi.edu

The non-destructive scanning of mail envelopes and packages is a topic of intense current interest. A large number of techniques are under investigation for the rapid screening of mail to detect illegal and/or harmful substances such as explosives, illicit drugs and bioterrorism substances such as the Anthrax causing bacterium Bacillus anthracis. Terahertz imaging has a number of important advantages in this application setting. Firstly paper, plastics, cardboard and many other packaging materials are largely transparent to THz radiation. Additionally, the coherent detection of THz pulses provides frequency-dependent, phase sensitive measurements of the response of the sample. This information may one day lead to a reliable method for the detection of specific substances in mail.

The chirped probe beam THz imaging system (CPTI) encodes the time varying THz information directly onto a chirped probe beam.[1] The chirped probe beam can be thought of as an optical pulse with a continuous frequency distribution, which is linear function of pulse delay. Therefore, the information at certain time is encoded at a corresponding frequency. By dispersing the probe beam in the frequency domain, the encoded information can be extracted.[2] The full THz waveform is measured simultaneously, thereby CPTI can dramatically accelerate the imaging speed.

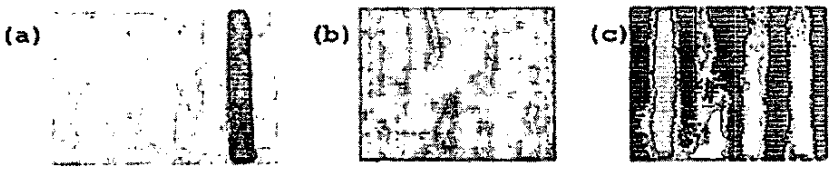

JMC2 Fig. 1. The powders used to demonstrate THz imaging. Figure (a) shows the piece of paper containing samples of salt, baking soda, flour and seasoning (from left to right). Figure (b) shows the THz image at a frequency of 0.3 THz. Figure (c) shows the results of classifying the THz data as described in the text. The image consists of five shades of gray. From darkest to lightest they correspond to paper, salt, baking soda, flour and seasoning.

We placed four different powdered samples: flour, salt, baking soda and seasoning inside a paper envelope and used the CPTI system to scan the envelope in x and y dimensions. This took approximately 8 minutes because we scanned the envelope in 2 dimensions. Using a 1D chirped probe pulse THz imaging system[3] it is feasible to attain a potential throughput of 12 envelopes/minute. 800 milligrams of each of the sample powders were placed on double sided cellotape and attached to a piece of paper as shown in Fig. 1(a) and placed in an envelope. The envelope was imaged and the transmitted THz waveform was measured at each pixel. The Fourier transform of the THz waveform provides information on the frequency dependent scattering, absorption and refractive index of the sample. In this way the powders can be detected. Figure 1(b) shows a THz image produced by plotting the intensity of the THz pulse at a frequency of 0.3 THz, in Fig. 1(c) we have used simple classification algorithms to differentiate between the different powders. A linear discriminant classifier was trained using the responses for 100 random pixels of each powder then the whole image was classified.

To more accurately assess the applicability of THz imaging to Anthrax detection we considered samples of Bacillus thurengiensis (BT) bacteria. Several bacilli produce spores that are physically and chemically very similar to those produced by B. anthracis, including B. thuringiensis, which is commonly used for insect control in gardens and is non-pathogenic to man and other mammals. Approximately 500 milligrams of B. thuringiensis spore flakes were placed inside an envelope and imaged using the CPTI system. Fig. 2. shows the envelope containing the BT spores and Fig. 3. shows the THz image of the envelope using the amplitude of the responses at 0.3 THz. The spores are clearly visible.

We have shown that THz imaging can detect powders inside envelopes at a concentration of 80 milligrams/cm^2 and that in a carefully controlled experiment classification algorithms can be used to differentiate between different types of powders. We have also presented images of bacteria spores inside envelopes and will demonstrate the performance of classification algorithms in detecting B. thuringiensis.

References

1. Z. Jiang and X.-C. Zhang, "Electro-optic measurement of THz field pulses with a chirped optical beam," *Applied Physics Letters* 72(16), pp. 1945–1947; 1998.
2. F.G. Sun, Z. Jiang, and X.C. Zhang, "Analysis of terahertz pulse measurement with a chirped probe beam," *Applied Physics Letters* 73(16), pp. 2233–2235, 1998.

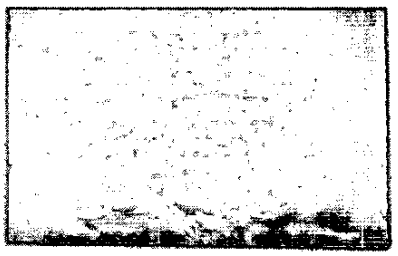

JMC2 Fig. 2. Standard optical photograph of the envelope containing the spore flakes. The envelope is backlit to allow the spore flakes to be viewed.

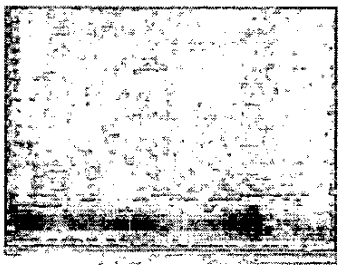

JMC2 Fig. 3. THz image of of the envelope containing the spore flakes. The amplitude of the responses at 0.3 THz were mapped to the grayscale intensity.

3. Z. Jiang and X.-C. Zhang, "Measurement of spatio-temporal terahertz field distribution by using chirped pulse technology," *IEEE Journal of Quantum Electronics* 36(10), pp. 1214–1222, 2000.

JMC3 **4:15 pm**

Three Dimensional Imaging Using T-ray Computed Tomography

Bradley Ferguson,[1,2,3] Shaohong Wang,[1] Doug Gray,[3] Derek Abbott,[2] and X.-C. Zhang,[1] [1]Department of Physics, Applied Physics and Astronomy, Rensselaer Polytechnic Institute, Troy, NY 12180, USA; [2]Centre for Biomedical Engineering and Department of Electrical & Electronic Engineering, Adelaide University, SA 5005, Australia; [3]CRC for Sensor, Signal and Information Processing, Technology Park, Mawson Lakes Boulevard, Mawson Lakes, SA 5095, Australia; Email: zhangxc@rpi.edu

For over a decade it has been known that terahertz time-domain spectroscopy systems can be

used to determine the frequency dependent optical properties of materials in the submillimeter wavelength regime. More recently 2 dimensional (2D) THz imaging systems[1,2] have been demonstrated for a diverse range of applications. However, using these imaging techniques the three-dimensional structure of the object has been unavailable until now. In particular the effects of variations in topography and the far-infrared optical properties of the sample have been indistinguishable.

T-ray computed tomography (T-ray CT) draws inspiration from the now ubiquitous X-ray CT system. The T-ray CT system hardware is a relatively simple extension of modern transmission mode THz imaging systems. A 2D image is obtained at a number of projection angles. This data can then be used to reconstruct the object in 3D.

The mathematical field of inverse problems for 3D image reconstruction is well established and a large number of potential algorithms exist for reconstructing the T-ray CT data. We have used the simple filtered backprojection algorithm to perform the inverse Radon equation[3] to reconstruct the object of interest. This method contains a number of implicit assumptions that are only approximately valid, but it serves to accurately reconstruct the simple samples that we have considered and demonstrates the power of this imaging technique. More accurate reconstruction algorithms are an important future research topic.

The reconstruction algorithm can be performed to reconstruct a number of features from the measured data depending on the desired application. To demonstrate the system a number of test samples were imaged and the 3D tomographic structure was extracted using the filtered backprojection technique. Figure 1 shows a plastic vial containing a plastic tube which was imaged using the T-ray CT system. A coarse sampling step of 1 mm in the x and y dimensions was used to obtain projection images for each 10° angular increment. The coherent nature of pulse THz systems was exploited and the timing information of the THz pulse for each projection was used to reconstruct the image shown in Fig. 2. The reconstructed image for 3 different heights are shown. The position of the plastic tube varies with each slice as it was placed at an angle. The brightness of the image is proportional to the reconstructed timing delay for each pixel, thus the brighter plastic tube can be seen to have a higher refractive index than the plastic vial wall. Figure 3 shows a 3D representation of the vial generated by combining all the horizontal slices the front of the vial has been cut away to show that the interior is accurately reconstructed.

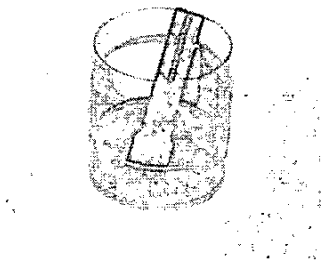

JMC3 Fig. 1. The vial and plastic tube used for testing the T-ray CT system.

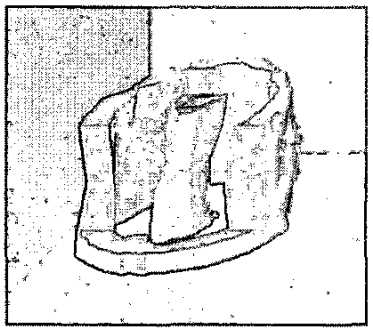

JMC3 Fig. 3. Reconstructed 3D image of the vial and plastic tube. Part of the data has been cut away to allow the interior of the vial to be viewed.

T-ray computed tomography imaging has significant potential in a number of applications. It is capable of reconstructing the 3D structure and frequency dependent far-infrared optical properties of an object. Using the reconstructed material properties different substances may be uniquely identified despite being hidden within other opaque structures. Applications of this technology are foreseen in non-destructive mail/packaging inspection, semiconductor testing, quality control of plastics and certain biomedical applications where the absorption of THz is not prohibitive.

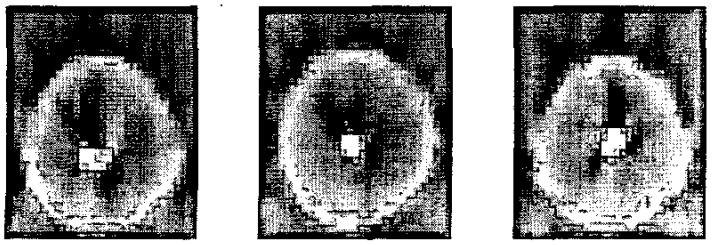

JMC3 Fig. 2. Reconstructed 2D slices of the vial and plastic tube. The reconstruction was performed for 3 slices. The image brightness reflects the refractive index of the sample at each pixel, lighter pixels correspond to higher refractive index.

References

1. B.B. Hu and M.C. Nuss, "Imaging with terahertz waves," *Optics Letters* 20(16), pp. 1716–1718, 1995.
2. Q. Wu, T.D. Hewitt, and X.-C. Zhang, "Two-dimensional electro-optic imaging of terahertz beams," *Applied Physics Letters* 69(8), pp. 1026–1028, 1996.
3. A.C. Kak and M. Slaney, *Principles of Computerized Tomographic Imaging*, Society of Industrial and Applied Mathematics, 2001.

JMC4 **4:30 pm**

Effect of Chirp in Diffraction of Short Electromagnetic Pulses through Subwavelength Apertures

Oleg Mitrofanov, Mark Lee, L.N. Pfeiffer, K.W. West, Bell Laboratories, Lucent Technologies, 600 Mountain Ave., Murray Hill, NJ 07974, Email: olegm@lucent.com

Frequency chirp of Terahertz (THz) pulses[1] has not been in the scope of researches yet. THz pulses generated using an ultrafast laser usually have very large bandwidth and the frequency chirp can be significant. As a result the frequency dependent phenomena develop noticeable chirp related effects in the time domain.

Recent studies of THz pulse coupling through an aperture of a THz near-field probe showed that the transmitted pulses experience spectral and temporal deformation.[2] In particular, a THz pulse generated by a photoconducting antenna appears compressed and temporally advanced due to transmission through a subwavelength aperture. The latter effect is determined by the negative frequency chirp of the THz pulses, which is typical for pulses generated in photoconductive switches.

Transmission through a small aperture is wavelength dependent. The coefficient varies by as much as an order of magnitude between 0.1 and 0.5 THz. Therefore broad-band THz pulses experience strong spectral and temporal deformation after propagation through the aperture. In a system that preferentially transmits shorter wavelengths, the chirp of the incident pulse defines whether the leading or the trailing edge of the pulse is suppressed after transmission. In the latter case, the transmitted pulse appears as advanced through the aperture.

To observe this effect, the diffracted pulse duration must be not larger than that of the incident pulse. A rapid change of the transmission coefficient within the pulse spectrum can cause spectral narrowing and, consequently, pulse spreading. Spectral deformation is schematically shown in Fig. 1 as a function of the aperture size. The transmission coefficient is assumed to vary as $\lambda^{-3/2}$ for $\lambda > 2d$,[3] and to remain constant for shorter wavelengths. The spectral amplitude of a typical THz pulse exponentially decreases with frequency. After the aperture, the spectral peak shifts to higher frequencies. The bandwidth of the pulse passes through its minimum and then increases as the aperture size decreases.

For experimental verification of the chirp effect, we compare transmission through a subwavelength aperture for chirped and unchirped THz pulses. The character of the THz pulses is controlled through the duration of the exciting optical pulse. The photocurrent rise time can be increased to a level of the decay time in the THz emitter, and the chirp of the THz pulse, therefore, minimized.

Fig. 2 shows waveforms of the THz pulses transmitted through a 10 μm aperture (emerged